



AXISYMMETRIC EXTRUSION TESTS ON CRUSHED ICE

Paul Spencer ¹

¹Ausenco Energy, Calgary, Alberta, CANADA

ABSTRACT

As part of the work done in the late 1980's to investigate the performance of the Molikpaq exploration structure to dynamic ice loads, axisymmetric extrusion tests were conducted. These tests involved a pair of rigid circular platens with a layer of previously crushed ice between the platens. The motion of the upper platen was controlled using a load test machine, total applied load and local pressures were measured along with various other parameters. The results of these tests were unfortunately not published. In this paper we present the data before it is essentially lost and/or forgotten. Various saw-tooth and smooth load waveforms were observed in this test program of 15 individual extrusion tests. Triaxial compression tests on crushed ice samples were also performed and these are discussed. These tests provide a useful addition to the publically available data on crushed ice extrusion.

INTRODUCTION

In 1987, a series of laboratory scale axisymmetric extrusion tests and triaxial compression tests were conducted on crushed ice. These were conducted by Geotech for Gulf Canada Resources as part of a project to investigate the dynamic response of the Molikpaq exploration structure to ice loads when located in the Canadian Beaufort Sea (Jefferies and Spencer, 1989). Unfortunately, the test results (Geotech, 1987) were not published by the test team and thus are generally unknown to the ice community. This oversight is now being rectified before the data is lost completely. The results of the subsequent laboratory scale plane-strain tests on crushed ice have been published by Spencer et al., (1992). At the time the axisymmetric tests were conducted, little information about the mechanical behavior of crushed ice at high confining pressures was available. In this paper, we discuss the tests and some observations resulting from them.

TRIAXIAL COMPRESSION TESTS

A set of triaxial compression tests were conducted on cylindrical samples of crushed freshwater ice. The crushed ice was prepared from block freshwater ice using an electric hand plane. The particle size distribution was determined from a sieve analysis of samples of the crushed ice. These results are presented in Table 1 showing the most probable particle size of approximately 150 micrometers. Note that particles larger than 850 micrometres were removed from the crushed ice source material by passing through a #20 sieve. The crushed ice material was then put into moulds 200mm high and 100mm in diameter and hand compacted in 8 to 16 lifts to reach the target densities in the range of 500kg/m³ to 700kg/m³. In general, the triaxial tests were conducted within 4 hours of sample preparation and were conducted at an ambient temperature of -10C.

Table 1. Ice Particle Size Distribution

Size Range (micrometers)	Weight Fraction
0 - 125	0.16
125 - 215	0.20
215 - 420	0.36
420 - 850	0.28

Details on the triaxial load test system can be found in Spencer et al. (1991). The testing procedure consisted of applying the confining hydrostat and then the deviatoric stress was applied under strain rate control. Tests were conducted at strain rates of between $1 \times 10^{-3} \text{ s}^{-1}$ and $2 \times 10^{-2} \text{ s}^{-1}$. A summary of the test data are given in Table 2. The stress strain curve was generally smooth but with a distinct kink or knee that was taken as the yield stress, indicated as point A in Figure 1. The ultimate yield stress is the maximum observed in the test except when the maximum deviatoric stress occurred at the end of the limit of the test axial displacement corresponding to a 15% axial strain, indicated as point B in Figure 1. Some difficulties in maintaining a constant confining pressure were experienced due to the large axial strains involved. The failure mode of the samples was either barrelling or change in dimensions of the right circular cylinder. Shear planes were not observed in these tests nor was tensile splitting observed. The sample density after application of the hydrostat was determined from measurements of the volume of fluid displaced from the test cell (Spencer et al., 1991). The final density was determined from direct physical measurement of the post-test samples.

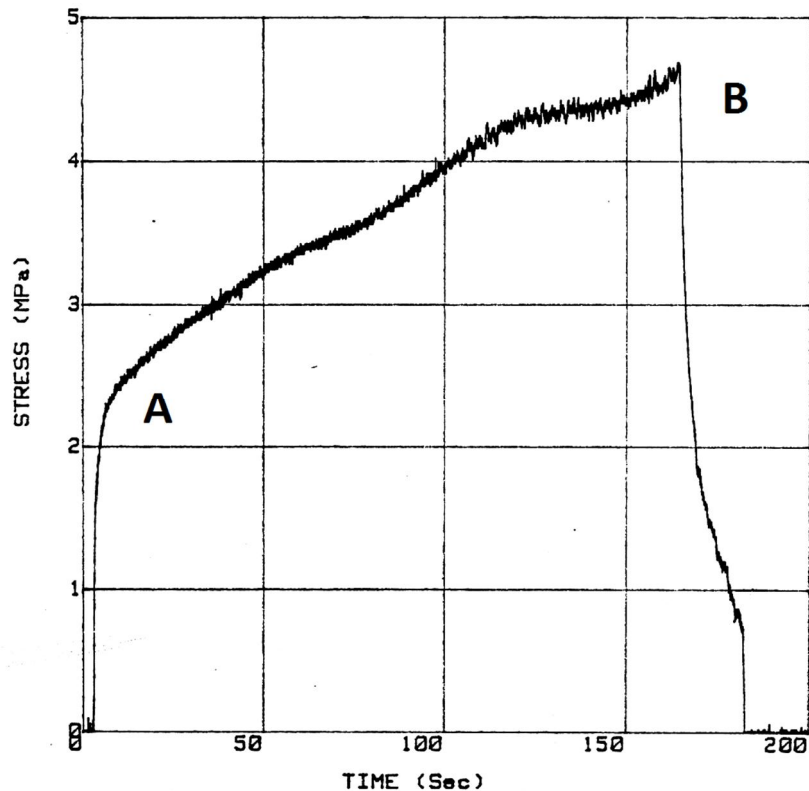


Figure 1. Time Series Deviatoric Stress data for T448

Table 2. Triaxial Test Results

Test	Strain Rate (s ⁻¹)	Confining Stress at Yield (MPa)	Yield Stress (MPa)	Confining Stress at Ultimate (MPa)	Ultimate Stress (MPa)	Initial Density (kg/m ³)	Density after hydrostat (kg/m ³)	Final Density (kg/m ³)
T443	1e-3	2.62	0.77	n/a	n/a	505	n/a	808
T446	1e-3	2.78	1.30	n/a	n/a	550	n/a	806
T448	1e-3	3.33	2.37	n/a	n/a	671	n/a	791
T449	1e-2	0.10	2.6	1.1	>4.7	702	n/a	760
T450	1e-2	3.1	2.7	3.1	7.4	695	771	815
T451	1e-2	9.4	3.6	9.4	8.2	707	825	841
T453	1e-2	18.4	5.5	18.4	8.4	670	n/a	865
T455	1e-2	10.3	4.1	15.0	7.6	697	738	833
T457	2e-2	19.2	4.9	19.2	8.1	689	818	811

The Yield Stress data are shown in Figure 2 as a function of confining pressure and as a function of initial density. Ultimate stress data are shown in Figure 3 along with a picture showing a post-test sample. The yield stress was represented as a Mohr-Coulomb material with Cohesion of 1.17MPa and Friction angle of 4.7deg. Figure 2 illustrates that there is an apparent linear trend between yield strength and initial sample density, there was little effect of yield stress on test strain rate. Figure 3 illustrates that the ultimate stress can also be represented as Mohr-Coulomb with Cohesion of 3.7MPa and Friction angle of 1.1deg.

Triaxial tests on crushed ice have also been conducted by Singh and Jordaan (1996). These authors also found that the strength was independent of strain rate and that the strength could be represented as a Mohr-Coulomb material.

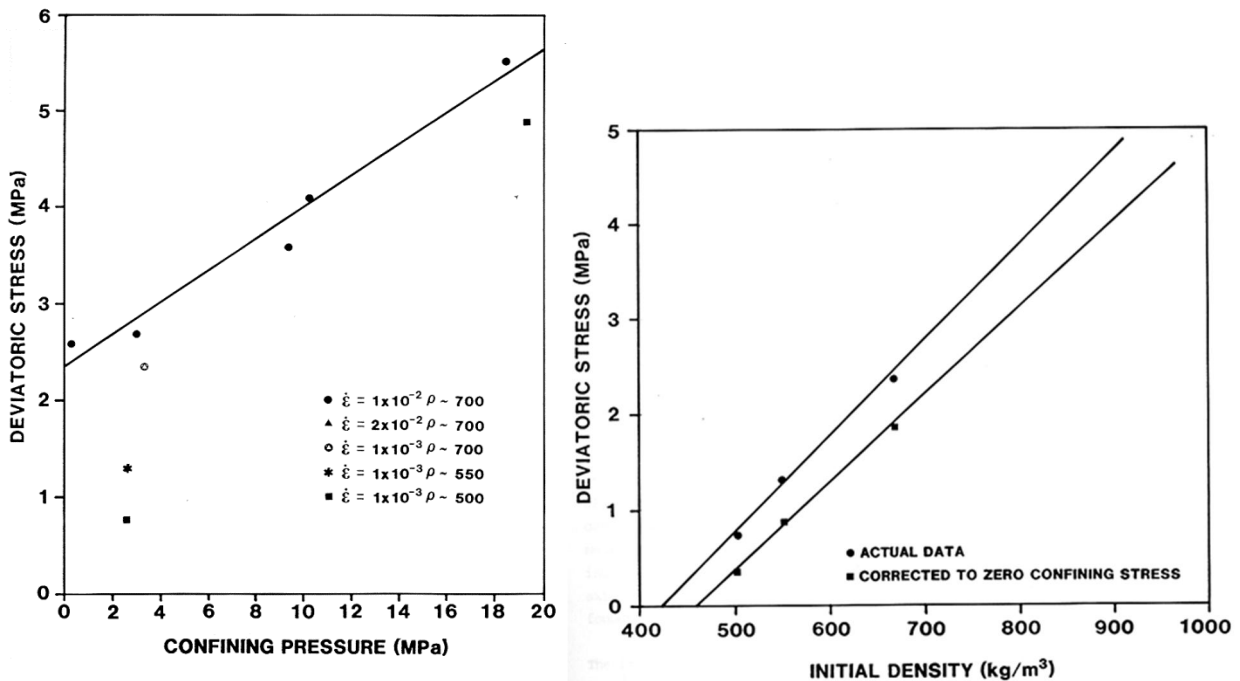


Figure 2. Yield Stress vs. Confining Stress (left) vs. Initial Density (right)

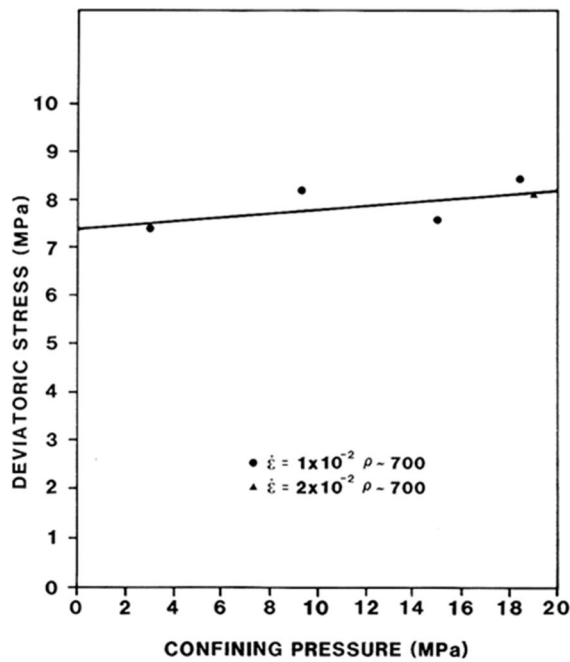


Figure 3. Ultimate Stress vs. Confining Stress and Sample after T451

PLATE EXTRUSION TESTS

The main purpose of the tests was to measure the mean applied pressure and radial pressure distribution during the extrusion of crushed ice. Tests were conducted at a temperature of -10°C . A 260mm diameter sample of crushed ice prepared using the same general procedure as for the triaxial tests was placed between two 270mm diameter uncoated steel platens. The upper platen was lowered under displacement control until either the load capacity of the equipment was reached (equivalent to about 9.7MPa pressure over the platen) or the test was manually terminated. The total applied load, displacement and local pressures were recorded during the tests. Unfortunately only relatively low capacity local pressure transducers were available for these tests (15MPa with 50% over-range capacity) and the centrally located pressure cell was overloaded during these tests and thus only data from the non-central local pressure cells were obtained. The diameter of the sensing area for these local pressure sensors was nominally 9mm. Some tests exhibited a smooth load-time curve and some tests exhibited a saw-tooth load time curve as illustrated in Figure 4. Figure 5 is a photograph capturing the ejection of material during an initial test. The velocity of the ejected material was estimated, based on simple ballistics, to be approximately 2m/s. The sample after a test is shown in Figure 6 showing a central zone of fused ice. The sample density at the end of some tests was determined from 27.6mm diameter sections. The test results are summarised in Table 3 where an "S" after the test identifier indicates the test was stopped prior to reaching the nominal 9.7MPa plate pressure. The general trends are illustrated in Figures 7 and 8.

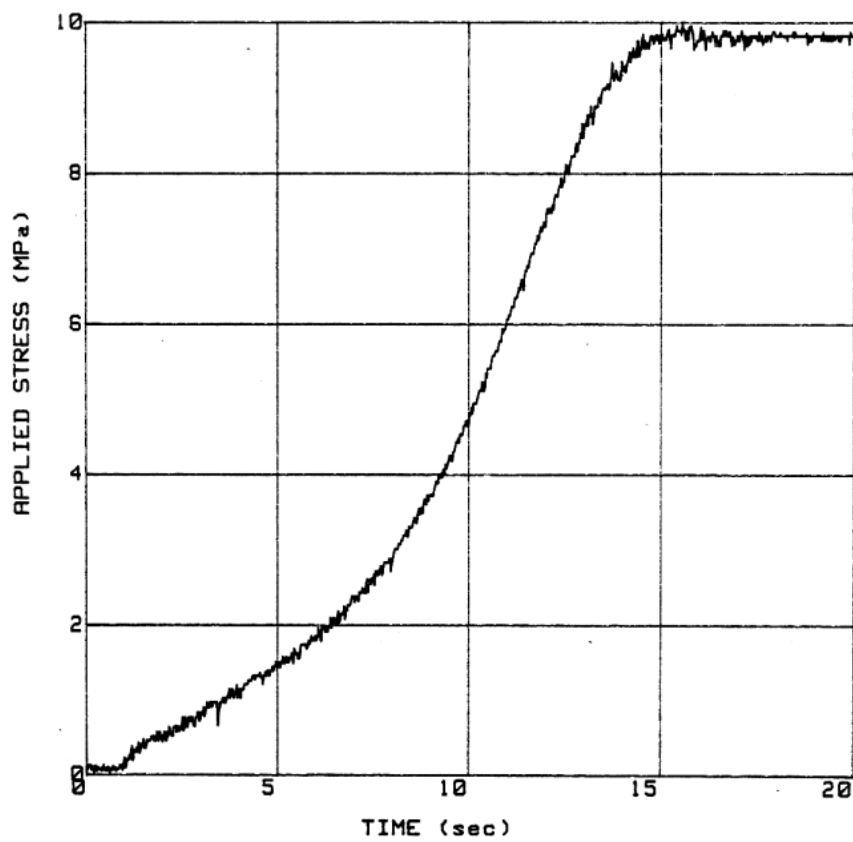
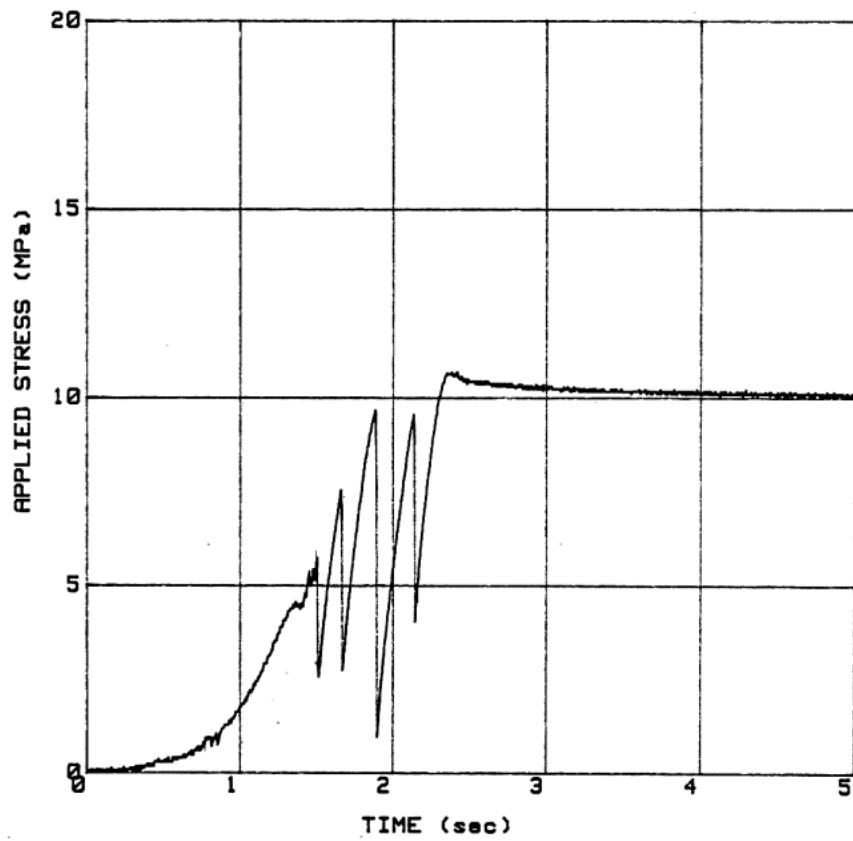


Figure 4. Saw-tooth Waveform (Test P042 top) Smooth Waveform (Test P035 bottom)

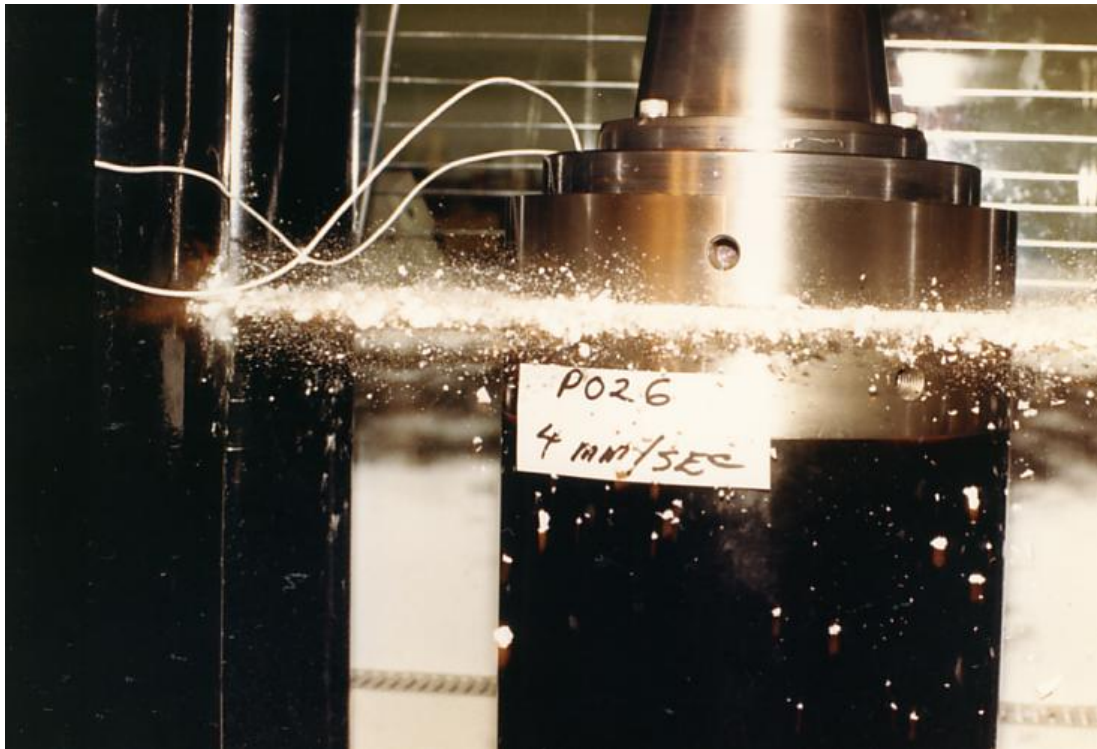


Figure 5. Ice Ejection during Plate Extrusion Test



Figure 6. Plate Extrusion Sample after Test

Table 3. Plate Test Results

Test	Initial Thick (mm)	Initial Density (kg/m ³)	Test Speed (mm/s)	Final Thick (mm)	Final Density (kg/m ³)	Radius for Density (mm)	Material Ejection
P030	25.4	610	3.90	4.77	n/a	n/a	Yes
P031	25.4	550	5.00	4.39	n/a	n/a	Yes
P032	25.4	537	0.53	10.19	855	65	No
P033	25.4	552	1.86	6.74	n/a	n/a	No
P034	25.4	512	3.16	7.41	n/a	n/a	Yes
P035	25.4	504	0.89	12.03	n/a	n/a	No
P036	25.4	519	0.16	14.36	818, 793, 775	15, 70, 110	No
P037	25.4	520	3.18	7.31	828, 812, 588	25, 65, 100	Yes
P038 S	25.4	512	3.38	10.95	858, 658, 558	20, 65, 110	No
P039	49.4	579	3.37	6.53	855, 822, 609	25, 70, 100	Yes
P040	12.7	632	2.09	6.50	834, 791, 618	25, 66, 100	No
P041	49.6	574	5.65	6.05	856, 740, 559	15, 70, 110	Yes
P042	12.7	553	3.52	4.70	808	20	Yes
P043 S	25.4	547	3.05	10.20	835, 634, 530	19, 66, 96	Yes
P044 S	25.4	521	3.05	21.96	619, 567, 533	20, 65, 84	No
P045 S	25.4	564	3.05	17.65	633, 565, 566	20, 65, 84	No
P046 S	25.4	568	3.05	7.37	787, 784, 608	15, 70, 110	No

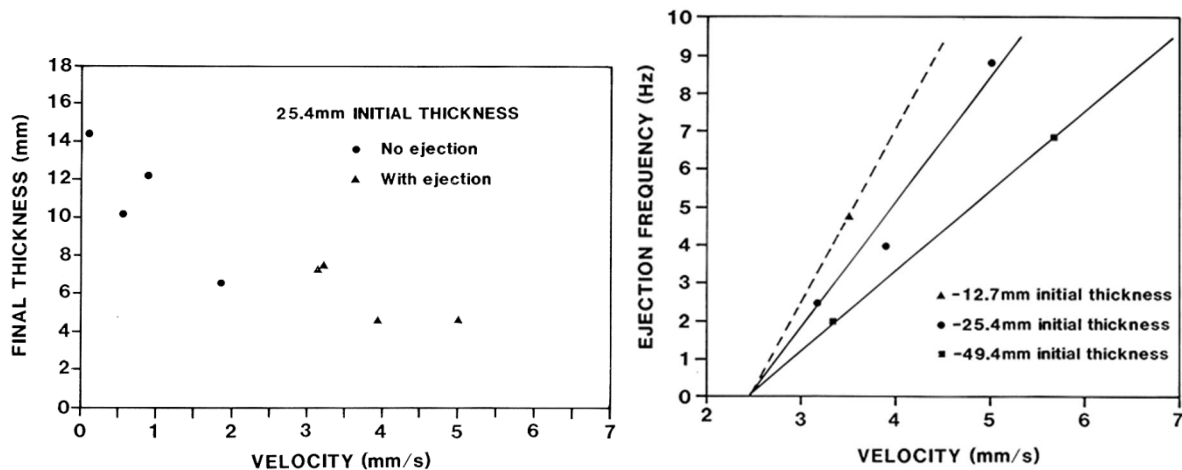


Figure 7. Final Layer Thickness (left) Saw-tooth frequency (right)

The final layer thickness for the tests that were not stopped is shown in Figure 7 and is seen to be an inverse function of the test speed. This indicates that for lower test speeds, the nominally 9.7MPa average pressure is reached at a larger crushed layer thickness. Also shown in Figure 7 is the observation that the saw-tooth behaviour only occurred at speeds greater than 2.5mm/s and that the frequency appears to be a linear function of test speed. The displacement per saw-tooth cycle varied from test to test and was in the range of 0.5mm to 1.5mm. The pressure distribution across the platen is shown in Figure 8. The central pressure was not observed but various estimates using the available data and load balance considerations, indicate that the central pressure was at least 50MPa. From Figure 8 the density at the end of the test shows that the central portion of the ice was compressed to high density and based on Figure 6 probably fused ice. The density was significantly less near the outer portions of the platen, the exception to the trend is shown in Figure 8 where Test P036

conducted at a low velocity of 0.16mm/s shows a more uniform density distribution across the platen than tests conducted at higher speed.

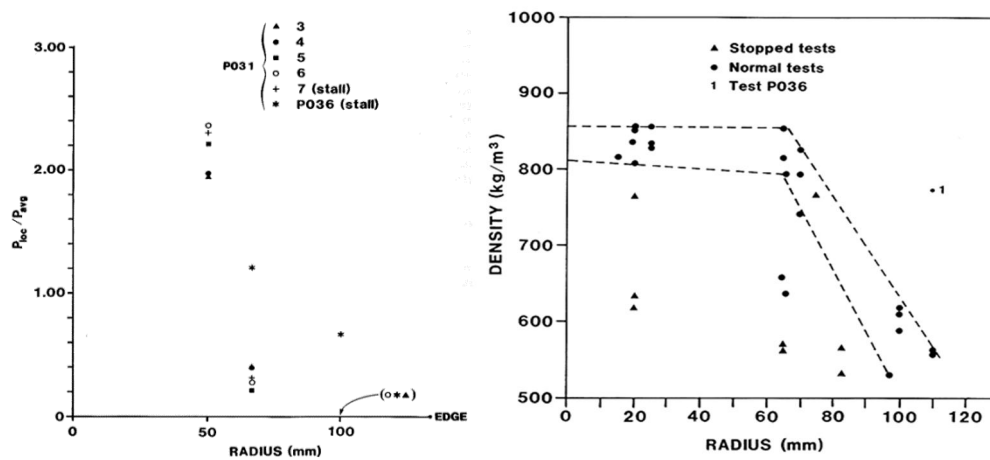


Figure 7 Local Pressure Distribution (left) Density Distribution (right)

The platen pressure was analysed and could be represented to be a power law on thickness. In some tests the exponent changed from when the layer thickness was large, ie Initial Conditions to when the layer thickness was small ie Final Conditions. These data are given in Table 4 where:

$$\text{Pressure(MPa)} = \text{Multiplier} * (\text{Thickness}/10\text{mm})^{\text{Exponent}}$$

Table 4. Platen Pressure Thickness Analysis

Test	Initial Thick (mm)	Initial Density (kg/m ³)	Speed (mm/s)	Initial Exponent	Initial Multiplier (MPa)	Final Exponent	Final Multiplier (MPa)
P039	49.4	579	3.37	-4.9	7.5	-4.9	7.5
P041	49.4	574	5.65	-3.9	5.1	-3.9	5.1
P037	25.4	520	3.18	-3.2	5.3	-3.2	5.3
P034	25.4	512	3.16	-4.5	46.4	-2.8	9.8
P035	25.4	504	0.89	-5.4	113.6	-5.4	113.6
P036	25.4	519	0.16	-5.4	93.0	-5.4	93.0
P040	12.7	632	2.09	-8.1	14.9	-5.1	8.3
P042	12.7	553	3.52	-20.6	578.0	-4.6	6.3

DISCUSSION AND CONCLUSIONS

Attempts were made to model the pressure thickness and pressure distribution trends in the extrusion tests as either a constant properties Mohr-Coulomb material or as a viscous fluid. While some success was achieved at lower pressures, neither model reproduced the large pressure end of the tests. Such modelling was developed and extended later for the plane strain tests on crushed ice (Singh et al., 1993).

Field tests using spherical indenters have been conducted on thick multi-year ice at Rae Point (Masterson et al., 1999) for various indentation speeds between 0.1 and 100mm/s. These field tests indicated that saw-tooth waveforms of varying frequency occurred at indentation speeds of greater than about 1.8mm/s. In the current tests a critical speed for saw-tooth waveforms of

2.5mm/s was found. Furthermore central pressures of up to 65MPa were measured in the field tests (Masterson et al., 1999), again similar to the 50MPa reported here.

There have been a number of field and scale laboratory tests which have revealed so called hot spots and spalling phenomena, see Gagnon (1999) for a review. These tests have generally started with intact ice, what the tests reported here show is that similar phenomena can also occur when the source material is crushed ice.

ACKNOWLEDGEMENTS

The author would like to thank the following people who directly worked on building the equipment and conducting the tests; Paul Spencer, Jim Lucas, Bill Graham and Rob Carlyon. Dan Masterson is acknowledged for useful discussions during the project and Mike Jefferies was instrumental in initiating the project and in getting the tests funded.

REFERENCES

Gagnon R.E., (1999), Consistent Observations of Ice Crushing in Laboratory Tests and Field Experiments covering Three Orders of Magnitude in Scale. POAC 1999 Vol 2 pp 858-869

Geotech (1987), Crushed Ice Laboratory Test Program, for Gulf Canada Resources, by Geotechnical resources ltd, 12 September 1987

Jefferies, M.G., and P.A. Spencer, (1989), Dynamic Ice/Structure Interaction with the Molikpaq at Amauligak I-65, Main Report, Volumes 1 and 2: Ice Loading of an Offshore Structure, Phase 1B: Dynamic Ice/Structure Interaction, Gulf Canada Resources Ltd., July.

Masterson, D.M., P. A. Spencer, D. E. Nevel, R. P. Nordgren (1999) "Velocity Effects from Multi-Year Ice Tests", 18th International Conference on Offshore Mechanics and Arctic Engineering (OMAE 99), St. John's, NF, July 11-16, 1999, Paper 99-1127

S. Singh, J. Xaou, I. J. Jordaan, P.A. Spencer (1993) "The Flow Properties of Crushed Ice", Proceedings of the 12th International Conference on Offshore Mechanics and Arctic Engineering, OMAE '93, Glasgow, Scotland, Vol. 4, pp 11-20

Singh. S., I.J. Jordaan (1996), Triaxial Tests on Crushed Ice. Cold Regions Science and Technology 24 (1996) 153-165

Spencer, P.A., D. M. Masterson and J.F. Dorris (1991), "The Measurement of Volumetric Strain in the Triaxial Testing of Ice Samples", Proceedings of the 10th International Conference on Offshore Mechanics and Arctic Engineering, 1991, Stavanger, Norway, Vol. 4, pp 237-244

Spencer, P.A., D. M. Masterson, J. Lucas and I.M. Jordaan (1992), "The Flow Properties of Crushed Ice: Experimental Observation and Apparatus", IAHR Ice Symposium 1992, Banff, Alberta, Vol. 1, pp 258-268